Journal of Neuroscience Methods 343 (2020) 108858

Contents lists available at ScienceDirect

Journal of Neuroscience Methods

journal homepage: www.elsevier.com/locate/jneumeth

Trading baseline with forelimbs somatosensory evoked potential for longitudinal analysis in thoracic transection spinal cord injury

Hasan Al-Nashash[a,**], Shiyu Luo[b], Xiaogang Liu[c,d], Angelo H. All[e,*]

[a] Department of Electrical Engineering, College of Engineering, ESB-2018, Engineering Science Building, American University of Sharjah, University City, Sharjah, 26666, United Arab Emirates
[b] Department of Biomedical Engineering, School of Medicine, Johns Hopkins University, Traylor Building, 720 Rutland Ave., Baltimore, MD, 21205, USA
[c] Department of Chemistry, Faculty of Science, National University of Singapore, Singapore
[d] The N.1 Institute for Health, National University of Singapore, Singapore
[e] Department of Chemistry, Faculty of Science, Hong Kong Baptist University, #844 Sir Run Run Shaw Building, Ho Sin Hang Campus, Hong Kong

ARTICLE INFO

Keywords:
Spinal cord injury
Transection
Somatosensory evoked potential
Longitudinal analysis
Rat

ABSTRACT

Patients who suffered from spinal cord injury (SCI) that come to healthcare professionals for diagnosis and treatment do not have electrophysiology baseline of somatosensory evoked potential (SSEP). The SSEP has always been used in research for data comparison to detect onset and severity of the SCI as well as for assessing its progress, endogenous and therapeutic recovery. This unmet need has motivated us to develop a new tool to substitute the baseline data with forelimb SSEP data of the same day. In this study, we report the development and investigation of three distinctive thoracic transections (right T10 hemi-transection (Rxl), left T8 and right T10 double hemi-transection (Dxl) and T8 complete transection (Cxl)) spinal cord injuries in an adult rat model. We used our well-established monitoring methods to obtain SSEP baselines as well as post-injury signals from days 4, 7, 14 and 21. We observed that spectral coherences obtained from non-injured spinal cord pathways are always above 0.8. The spectral coherence is dimensionless measure with values between 0 and 1 and measures the correlation between two time signals in the frequency domain. Analysis of variance (ANOVA) results also showed that there is a significant difference between the spectral coherence componanet means before and after injury with reaching $p = 0.05$ for Rxl, $p = 0.02$ for DxI, and $p = 0.00$ for CxI. Our signal processing enables us to replicate comparable detection of the natural history of injuries longitudinally without the implication of baseline SSEP signals, highlighting the potential of this analysis method for clinical studies.

1. Introduction

In translational research projects, like spinal cord injury (SCI), objective assessments are key for translating the results into clinical applications. Electrophysiological monitoring, such as somatosensory evoked potential (SSEP) plays a pivotal role in most neuroscience studies. Over the past decade, we have used SSEP recording and various forms of novel signal processing to investigate onset, progress and endogenous recovery in thoracic contusion and transection SCI models. However, in real life, patients suffering from SCI do not come with pre-recorded baselines. This unmet clinical challenge has motivated us to develop a more realistic and applicable alternative. Here, we describe an innovative procedure that uses somatosensory signals from non-injured pathways projecting above the injury level, like forelimbs, as a reference for comparison, which can eliminate the need for hindlimb baseline signals. Our results obtained from the right hemi-transection, double hemi-transection, and full transection subject groups show that forelimbs SSEP data can reliably be used to study the natural history of SCI.

Spinal cord injury, characterized and defined by the disruption of sensory and motor neural signal conduction and neuronal damage, can often lead to various degrees of functional loss below the lesion site (Agrawal et al., 2008; Maynard et al., 1997). In most cases, SCI incurs significant costs for individuals and the social system. Despite the rising level of care for SCI patients in recent years, the life expectancy of people with SCI is still lower than that for the healthy population in the corresponding age group (Ahuja et al., 2017; Lee et al., 2014; New et al., 2014; Krause and Saunders, 2011). The severity of the problem

* Corresponding author at: Department of Chemistry, Faculty of Science, Hong Kong Baptist University, #844 Sir Run Run Shaw Building, Ho Sin Hang Campus, Hong Kong.
** Corresponding author.
E-mail addresses: hnashash@aus.edu (H. Al-Nashash), sluo15@jhu.edu (S. Luo), chmlx@nus.edu.sg (X. Liu), angelo@hkbu.edu.hk (A.H. All).

https://doi.org/10.1016/j.jneumeth.2020.108858
Received 18 February 2020; Received in revised form 2 June 2020; Accepted 8 July 2020
Available online 09 July 2020

calls for improved methods of SCI assessments, diagnosis and treatment.

Somatosensory evoked potential (SSEP) is considerd to be a promising parameter for objective evaluation, offering continuous monitoring of SCI (All et al., 2010). SSEP is the evoked electrical potential recorded in the brain in response to peripheral stimulation, making it an ideal candidate for evaluating somatosensory system function, and by extension, spinal cord integrity (Agrawal et al., 2010). SSEP has been adopted widely in clinical settings for surgeons to continuously monitor signs of abnormality during surgeries that might compromise the spinal cord (Bazley et al., 2014; Nuwer, 1998; Maybhate et al., 2012), which can be recorded continuously in real-time and could be easily extended into long-term observation. As a direct assessment of the integrity of the ascending sensory pathway, SSEP also provides a more sensitive measurement into the progression of SCI (Vipin et al., 2016).

In SCI research, time-domain SSEP analysis is often adopted to track the progression of SCI. In these cases, features such as latency and peak amplitude are processed and monitored (Agrawal et al., 2008; Jung et al., 2002; Kong and Thakor, 1996). However, after SCI, the shape of the SSEP signals would be significantly altered, rendering it difficult to determine the signal onset and peaks. This challenging signal processing step is further compounded by the lack of baseline data in clinical settings. Unlike under research settings, SSEP data recorded before traumatic SCI are almost invariably unavailable (Al-Nashash et al., 2009). Traditional SSEP-based SCI assessment have relied on signal processing techniques auch as autoregressive modeling, adaptive latency measurement and knimatic measures to address the difficulty in locating signal peaks and latency trends (Jung et al., 2002; Cerutti et al., 1988). However, these methods do not allow the critical comparison between cortical response recordings made through stimulation of different limbs. More recent attempts to resolve this challenge proposed additional methods including SSEP linear signal modeling (Mir et al., 2018), the signal morphological difference (Mir et al., 2011) and signal amplitude histogram analysis (Mir et al., 2010). Despite the apparent success of these methods, they have too many parameters to adjust. The spectral coherence method, on the other hand, is robust and does not require any adjustment of signal parameters nor does it require a priori knowledge of signal amplitudes or latency variations. Spectral coherence is the square of the cross power spectrum between two signals divided by the power spectrum of the two spectra, respectively (All et al., 2007). The adoption and improvement of these analysis methods would facilitate better objective post-SCI assessments.

The goal of this study is to demonstrate the feasibility of using SSEP as the monitoring method in SCI cases, without the need for baseline SCI data. In this paper, we intended to establish the generalization of the spectral coherence analysis of SSEP in rodent transection SCI model.

2. Materials and methods

2.1. Animals

We followed the guidelines published in the Rodent Survival Surgery Manual for our *in vivo* experimental designs (Flecknell, 2016; Bernal et al., 2009; Grimm et al., 2015; Waynforth, 1980). All the *in vivo procedures* were also reviewed and approved by the Institutional Animal Care and Use Committee (IACUC) at the National University of Singapore. Twenty adult male and female Sprague-Dawley rats (200 − 225 g) from Charles River Laboratory were randomly assigned to four experimental groups (n = 5), composed of three thoracic (T) transection injury groups: right T10 hemi-transection (Rxl), left T8 and right T10 double hemi-transection (Dxl), T8 complete transection (Cxl) and one control, which received only laminectomy without any injury. Laminectomies as well as transection injuries, which were performed by one clean, sharp transverse incision using a small-size scalpel, were done under a microscope. Using a water heating pump, we kept the rats' body temperature unchanged at 37 +/- 0.5 °C during the entire surgical and monitoring procedures. We employed intraperitoneal (ip) injection of 0.2 − 0.3 ml freshly mixed cocktail of Ketamine (50 mg/kg), Xylazine (5 mg/kg) and Acepromazine (1 mg/kg) to both induce and maintain general anesthesia. We periodically examined the response to noxious stimuli to avoid causing pain in rats undergoing surgery and never observed any form of positive reflex or response to pain stimuli, confirming their adequate general anesthesia throughout the entire surgical and monitoring procedures. None of the rats needed to be euthanized early due to pain, suffering or surgical complications.

2.2. SSEP electrode implantation

The SSEP electrodes were implanted at least 7 days before the injury day to allow the rats to recover. During this period, the SSEP signals were also monitored to verify their quality and to obtain the SSEP baselines. We also examined any potential side effect of intra-cranium electrode implantation on rats' overall health. General anesthesia was induced on rats - a midline skin incision was performed on and their skulls were cleaned. A micro drill (Ideal Micro Drill; Cellpoint Scientific, Inc) was used to make tight holes by gently drilling on the skull bone. Two small holes on the left and right hemispheres at 0.2 mm posterior and 3.8 mm lateral to the bregma for the forelimbs SSEP recordings and two holes on the left and right hemispheres at 2.5 mm posterior and 2.8 lateral to the bregma for the hindlimbs SSEP recordings were drilled and four transcranial stainless-steel screw electrodes (E/363/20/SPC; Plastic One, Inc) were placed on them. The fifth hole for the reference electrode was drilled in the right hemisphere at 3.0 mm lateral to lambda. All five electrodes had very light contact with the dura matter without irritating the structures and or applying pressure on the brain. To fix the position of these electrodes permanently and enable longitudinal SSEP recordings from the same spot and to cover the exposed skull, a small amount of dental cement (Jet Denture Repair Package; Lang Dental Manufacturing Co., Inc) was delicately poured on the sites. It is noteworthy that none of these procedures was found to be harmful to rats. The position of electrodes, signs of infection and presence of any other complications were verified by the histological examinations post-mortem as well.

2.3. Transection SCI

After inducing general anesthesia, we performed a dorsal midline skin incision to expose thoracic vertebrae and used No. 11 scalpel (Swann-Morton) to carefully retract paravertebral muscles around the lamina from T7 to T9 for T8 laminectomy and transection injury and from T9 to T11 for T10 laminectomy and transection injury under Nikon operating microscope (SMZ745 T; Nikon Corporation). Laminectomy is a simple procedure, with minimal bleeding, to expose the dorsal part of the spinal cord safely, which causes no complication post-surgery. Each complete or hemi-transection was verified meticulously using the microscope to ensure the perfection and consistency among all rats. In the case of hemi-transections, we visually referenced the dorsal midline of the spinal cord and then performed one clean cut transversally by inserting the scalpel perpendicularly into the spine parenchymal. For the complete transection, the diameter of the spinal cord on the transverse plane was completely cut without damaging surrounding tissue (Vipin et al., 2016; All et al., 2019).

2.4. Post-operative animal care

The para-vertebrae muscles were sutured back to their anatomical position carefully and the skin was closed soon after the injury. The povidone-iodine pad was used to clean the site of skin-incision and rats' body temperature was kept at 37 ± 0.5 °C promptly and for the next 2 h using a heating pat. The bladder of the rats was emptied manually twice a day until they regained their normal urination function. Subcutaneously analgesic buprenorphine (0.06 mg/kg) and antibiotic

gentamicin (8 mg/kg) were given for 5 days.

2.5. Multi-limb SSEP recording

Our well-established SSEP setup components, manual procedures, monitoring tasks and signal processing were reported extensively in our previous studies (Vipin et al., 2016; All et al., 2019; Bazley et al., 2011, Bazley2012; Vayrynen et al., 2016). (a) Screw electrodes (E363/20, Plastics One, Inc., Roanoke, VA) to be implanted on the skull, (b) an isolated current stimulator (Letchworth DS3; Digitimer Ltd., Welwyn Garden City, UK) used to deliver well-calibrated stimulations to a pair of stainless steel subdermal needle electrodes (RI Safelead F-E3 − 48; Grass Technologies, West Warwick, RI) inserted into each limb, (c) a Tucker-Davis Technologies (TDT; Tucker-Davis Technologies Inc., Alachua, FL) state-of-art workstation with a 64-channel head-stage amplifier (RA64LI) for SSEP monitoring, (d) a low-noise digital pre-amplifier (RA4PA), and (e) a Bio-amplifier processor (RZ5) used to complete data acquisition system. Actual SSEP signals were visually monitored continuously in real-time. Although preliminary signal processing was done in real-time, we executed a comprehensive novel analysis offline as well (Agrawal et al., 2010; Bazley et al., 2014; Agrawal et al., 2009).

The skull screw electrodes were connected to an amplifier. Pairs of subdermal needle electrodes were placed near the Median and Tibial nerves (without direct contact with the nerves) in both forelimbs and hindlimbs. The OpenEx software controlled the stimulator. The stimulator was individually triggered from the Bioamp processor at 0.5 Hz to deliver the stimuli (3.5 mA pulse intensity, 200 μsec pulse width at 1 Hz) into the subdermal needle with this specific order: “right forelimb, left forelimb, left hindlimb, right hindlimb and back to the right forelimb”. The same order was repeated throughout the experiment. Upon each limb stimulation, simultaneous SSEP signals were recorded by the TDT workstation from all four cortical electrodes in 1-sec epochs at a sampling rate of 4882 Hz via the amplifier and data acquisition setup. This enabled us to collect 150 samples of SSEPs of 1-sec length each from corresponding somatosensory cortices upon stimulation of 150 positive monophasic pulses delivered consecutively to each one of the four limbs.

As we reported previously, Isoflurane gas anesthesia is found to be the most desirable for use in SSEP recordings. Intra-peritoneum and or intra-muscle injection of other anesthetic agents like Ketamine will not be suitable for SSEP recording (though they are excellent methods for motor evoked potential MEP recordings) (Agrawal et al., 2009; Iyer et al., 2010). We used a Patterson Scientific Versa II isoflurane vaporizer (Patterson Scientific, Foster City, CA) to deliver a mixture of 1.5 % isoflurane (Singapore Aerrane Isoflurane; Baxter Healthcare, Singapore), 90 % oxygen, and room air at the flow rate of 1.5 L per minute to all rats, through an anesthesia mask connected to a diaphragm with a C-pram circuit, which was maintained well-controlled and strictly unchanged for the entire duration of signal recording. With the help of a rodent heating pad, rats’ body temperature was also kept uniform at 37 °C during the entire SSEP recording session. In addition to the need for comparable SSEP data among all subjects, keeping anesthesia level and body temperature constant in all rats is critical since any fluctuation of either of the two could also cause significant changes in the quality of the SSEP signals. Rats were moved into a Faraday cage to avoid surrounding environment artifacts, as well as 60 and 120 Hz noise during SSEP recordings.

SSEP signals were recorded 5–7 days after skull screw implantation from healthy rats and prior to the injury. This is to verify that (i) electrodes are functional especially after the acute phase of surgical procedures and (ii) to obtain the baseline data that would eventually be used for comparisons in signal processing later. The same procedures were followed for SSEP recordings on day 4, day 7, day 14 and day 21 post-SCI.

2.6. Definitions

We will be using the following notations. **RxI:** Right T10 hemi-transection injury; **DxI:** Left T8 and Right T10 double hemi-transection injury; **CxI:** T8 complete transection injury; **RxS:** Right forelimb and hindlimb stimulation; **LxS:** Left forelimb and hindlimb stimulation; **RxR:** Right hemisphere SSEP cortical recording; **LxR:** Left hemisphere SSEP cortical recording.

2.6.1. Signal processing

In this work, we used spectral coherence to measure the spectral correlation between forelimbs and hindlimbs SSEP signals. Spectral coherence is a normalized cross-power spectrum computed between two signals such as the SSEPs recorded from the scalp following forelimbs and hindlimbs stimulations. This method has many advantages including being a normalized objective and quantitative measure with values ranging between 0 and 1. In addition, it does not require trained examiners and can use the forelimb SSEP of any day following the injury instead of the baseline hindlimb SSEP.

All signal processing was performed in MATLAB R2018b from MathWorks Inc. The SSEP signal was first band-passed with bandwidth 20 Hz to 1KHz. The power line interference was reduced using a notch filter. To improve the signal-to-noise ratio (SNR) of the SSEP signals, we performed ensemble averaging. Windows of 260 msec of the averaged

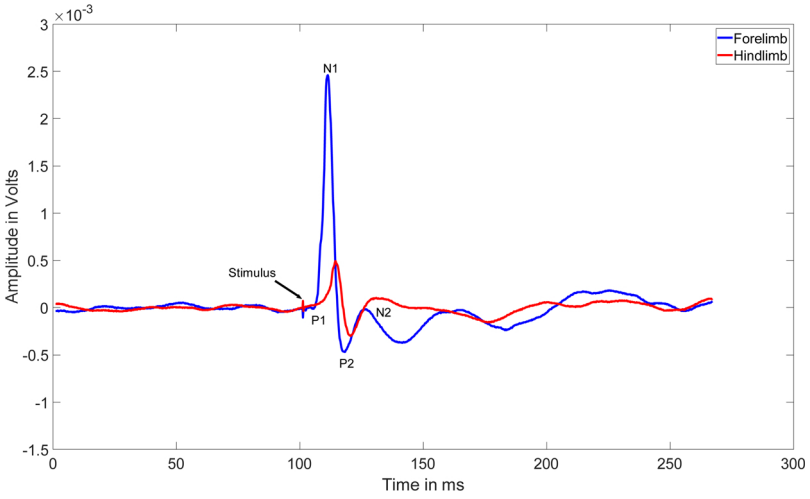

Fig. 1. Examples of forelimb and hindlimb recordings recorded during baseline.

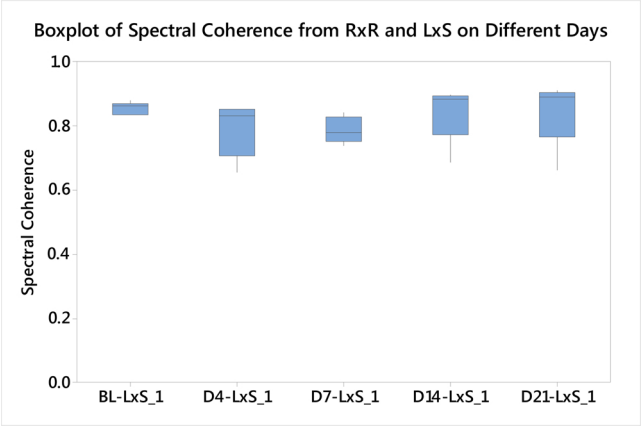

Fig. 2. Average Spectral Coherence from right hemisphere recording (RxR) with left forelimb and hindlimb stimulation (LxS) on different days for Right T10 hemi-transection injury (RxI).

SSEP signals recorded following forelimb and hindlimb stimulations were used for computing the spectral coherence. Fig. 1 shows examples of forelimb and hindlimb recordings recorded before the injury. The averaged SSEP signals were obtained by averaging 712 SSEPs from one animal.

2.6.2. Spectral coherence

Spectral Coherence is a real-valued quantitative measure of the correlation between two time signals in the frequency domain. In this research, the two signals are the average SSEP signals (x and y) recorded from the scalp following forelimb and hindlimb stimulation respectively. Technically, the spectral coherence between time signals x and y is the normalized cross-power spectrum computed between the two signals (Al-Nashash et al., 2009; All et al., 2007; Fatoo et al., 2007) and is defined:

$$\gamma_{xy}(f) = \frac{|P_{xy}(f)|^2}{P_{xx}(f)\,P_{yy}(f)}$$

Where, $P_{xy}(f)$ is the cross-power spectrum between x and y signals, $P_{xx}(f)$ is the auto-power spectrum of signal x, and $P_{yy}(f)$ is the auto-power spectrum of the signal y. The spectral coherence is dimensionless with values between 0 and 1. A spectral coherence of 1 means that cross-correlation between x and y have full spectral overlap and the two signals are similar. On the other hand, if spectral coherence is 0, this means that x and y are completely unrelated with no spectral overlap between them. In practice, the coherence function is usually greater than 0 and less than 1.

The spectral coherence recorded from forelimb and hindlimb SSEPs during baseline was reported in a previous study (All et al., 2007). It was observed that relatively high spectral coherence values were observed in the range DC–200 Hz with a peak value at a frequency of 150 Hz (Sherman et al., 2010). Similar results were found in this study. Hence, in this research, we calculated the mean spectral coherence value from the frequency band below and above 150 Hz. The frequency band was determined from the frequencies at which spectral coherence drops by -3 dB from peak value and this band was found to be 75–225 Hz.

2.6.3. Statistical analysis

The statistical software package Minitab® 18.1 was used for statistical data analysis. Statistical analysis was performed on spectral coherence data over 5 time points: baseline (BL), day 4 (D4), day 7 (D7), day 14 (D14) and day 21 (D21). The mean, standard deviation (StDev), range, median, lower and upper quartiles (Q1 and Q3) of spectral coherence values were calculated for the available data recorded from the three types of injury data: RxI, DxI and CxI. We compared the spectral coherence data using a simple main-effect analysis of variance (ANOVA) on data obtained from all animals of all three injury groups with both left and right forelimb and hindlimb stimulation. No animals were excluded in this analysis. The null hypothesis for a certain injury type was that the means of the corresponding spectral coherence are equal on all days.

3. Results

In this research, we randomly divided the male and female animal subjects into three injury groups and one control group. The three groups are right hemi-transection at T10 (RxI); left T8 and right T10 double hemi-transection (DxI); and complete transection at T8 (CxI). Note that the ascending sensory pathways originating from forelimbs, which are above the injury sites, reaching the brainstem and then decussating to corresponding somatosensory cortices will remain intact. Hence, the SSEP signals recorded from forelimbs were used to replace the baseline hindlimb SSEP signals.

Following ensemble averaging of both forelimb and hindlimb SSEPs, spectral coherence is performed as described earlier. Fig. 2 shows the spectral coherence boxplot values calculated from SSEPs recorded from the right hemisphere with left forelimb and left hindlimb stimulation on different days for all animals who had right hemi transection injury (RxI). The SSEP spectral coherence data statistics for RxI with LxS are shown in Table 1.

The mean spectral coherence value obtained before an injury during baseline is approximately 0.85. Results also indicate that spectral coherences on the days following injury are similar to the baseline and of values above or equal to 0.8. The figure also shows that spectral coherence recorded from stimulating left limbs are unaffected by RxI.

Fig. 3, on the other hand, shows the spectral coherence mean recorded from the left hemisphere with the right forelimb and right hindlimb stimulation on different days for the right hemi transection injury (RxI). The SSEP spectral coherence data statistics for RxI with RxS are shown in Table 2.

The mean spectral coherence value of baseline, obtained before the injury, is above 0.82 close to what we had earlier in Fig. 2. However, unlike what reported in Fig. 2 above, results on the days following injury indicate that spectral coherences on most days drop below 0.7 and reaching 0.6 on day 4, which reflects clearly the ground truth of RxI.

The above comparison between spectral coherence before and after injury was repeated for all three types of injury. Fig. 4 shows the spectral coherence mean recorded from the left hemisphere with right forelimb and right hindlimb stimulation on different days for all three types (Rxl, Dxl and Cxl) of injury. The SSEP spectral coherence data statistics for DxI and CxI are shown in Table 3 and Table 4 respectively.

Results indicate that in the case of DxI and CxI, the mean spectral coherence for all animals drops down to less than 0.3 and 0.1 respectively. These very low spectral coherence values indicate that hindlimb ascending sensory pathways were severely disrupted with the possibility of double or complete spinal cord injury in agreement with the ground truth. Furthermore, for all animals in all types of SCI experiments, the spectral coherence before injury always shows values above

Table 1
SSEP spectral coherence data statistics obtained from right hemisphere recording (RxR) with left forelimb and hindlimb stimulation (LxS) on different days for Right T10 hemi-transection injury (RxI).

Day/Variable	Mean	StDev	Q1	Median	Q3	Range
BL-LxS	0.85	0.02	0.83	0.86	0.87	0.05
D4-LxS	0.79	0.08	0.71	0.83	0.85	0.20
D7-LxS	0.79	0.04	0.75	0.78	0.83	0.10
D14-LxS	0.84	0.09	0.77	0.88	0.89	0.21
D21-LxS	0.85	0.11	0.77	0.89	0.91	0.25

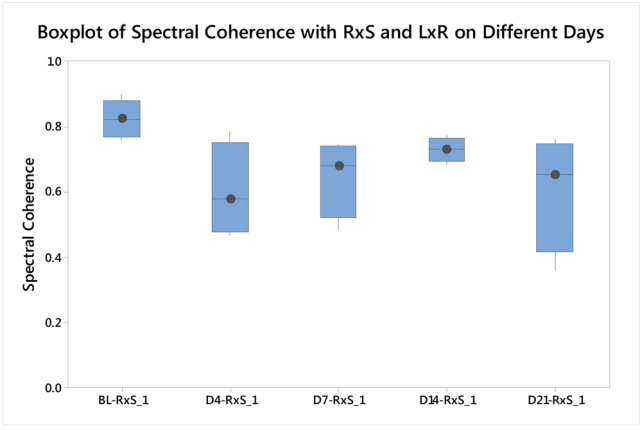

Fig. 3. Average Spectral Coherence from left hemisphere recording (LxR) with right forelimb and hindlimb stimulation (RxS) on different days for Right T10 hemi-transection injury (RxI).

Table 2
SSEP spectral coherence data statistics obtained from from left hemisphere recording (LxR) with right forelimb and hindlimb stimulation (RxS) on different days for Right T10 hemi-transection injury (RxI).

Day/Variable	Mean	StDev	Q1	Median	Q3	Range
BL-RxS	0.82	0.06	0.77	0.82	0.88	0.14
D4-RxS	0.60	0.15	0.48	0.58	0.75	0.32
D7-RxS	0.65	0.12	0.52	0.68	0.74	0.26
D14-RxS	0.73	0.04	0.69	0.73	0.77	0.09
D21-RxS	0.61	0.18	0.42	0.65	0.75	0.40

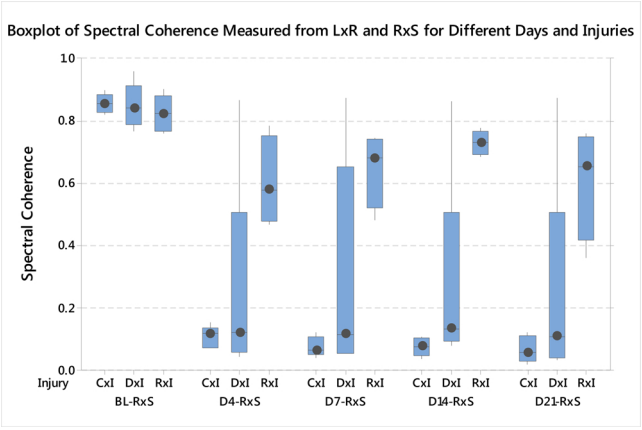

Fig. 4. Average Spectral Coherence recorded from left hemisphere with right forelimb and hindlimb stimulation on different days for three injury groups including Right T10 hemi-transection injury (RxI), Left T8 and Right T10 double hemi-transection injury (DxI) and T8 complete transection injury (CxI).

Table 3
SSEP spectral coherence data statistics obtained from Double hemi-transection injury (DxI) with Right forelimb and hindlimb stimulation (RxS).

Day/Variable	Mean	StDev	Q1	Median	Q3	Range
BL-RxS	0.85	0.07	0.79	0.84	0.91	0.19
D4-RxS	0.25	0.35	0.06	0.12	0.51	0.82
D7-RxS	0.31	0.35	0.06	0.12	0.65	0.82
D14-RxS	0.27	0.34	0.09	0.14	0.51	0.78
D21-RxS	0.24	0.36	0.04	0.11	0.51	0.84

Table 4
SSEP spectral coherence data statistics obtained from from Complete transection injury (CxI) with Right forelimb and hindlimb stimulation (RxS).

Variable	Mean	StDev	Q1	Median	Q3	Range
BL-RxS	0.86	0.03	0.83	0.85	0.88	0.08
D4-RxS	0.11	0.03	0.07	0.12	0.14	0.08
D7-RxS	0.08	0.03	0.05	0.06	0.11	0.08
D14-RxS	0.08	0.03	0.05	0.08	0.11	0.07
D21-RxS	0.07	0.04	0.03	0.06	0.11	0.10

Table 5
Longitudinal Model Analysis Results.

Injury Type	Source	DF	Adj SS	Adj MS	F-Value	P-Value
No Injury	Days	4	0.021	0.005	0.92	0.470
	Error	20	0.113	0.005		
	Total	24	0.134			
RxI	Days	4	0.162	0.040	2.93	0.050
	Error	16	0.221	0.014		
	Total	20	0.382			
DxI	Days	4	1.373	0.343	3.51	0.025
	Error	20	1.954	0.098		
	Total	24	3.327			
CxI	Days	4	2.390	0.597	507.80	0.000
	Error	20	0.024	0.001		
	Total	24	2.413			

0.8.

Statistical analysis of spectral coherence values revealed different progression of injury across the three injury groups. Based on spectral coherence analysis, the right hemi-transection, double transection, and full transection groups exhibited different progress of injury patterns as well as modes of recovery. We performed ANOVA analysis for each injury type separately. We compared the spectral coherence between data groups obtained on all different days. We did not perform analysis between BL and D4 separately or between BL and D7. We performed longitudinal model analysis in which all time points (factor) are modelled in the same analysis. The model results are shown in Table 5.

Fig. 5 shows the interval plot of the Spectral Coherence from the left hemisphere recording with the right forelimb and right hindlimb simulation of RxI vs days before and after injury with a 95 % confidence interval.

ANOVA results demonstrated that there is a significant difference between these means ($p = 0.05$) and reject the hypothesis of equal means. When compared with analysis results without injury, $p = 0.47$ where the null hypothesis is accepted reflecting the fact that there is no

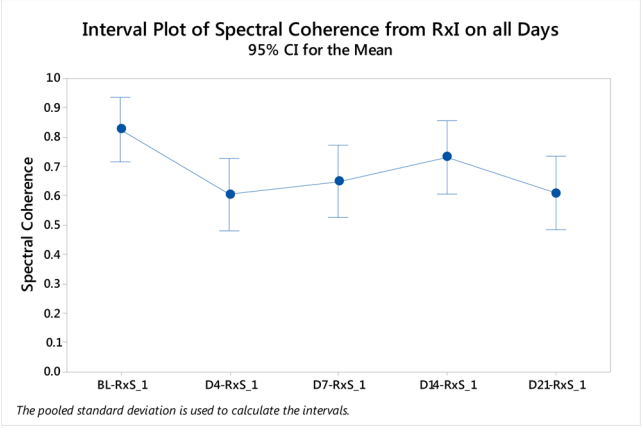

Fig. 5. Interval plot of the Spectral Coherence from the left hemisphere recording with right forelimb and hindlimb simulation of RxI vs days before and after injury with a 95 % confidence interval.

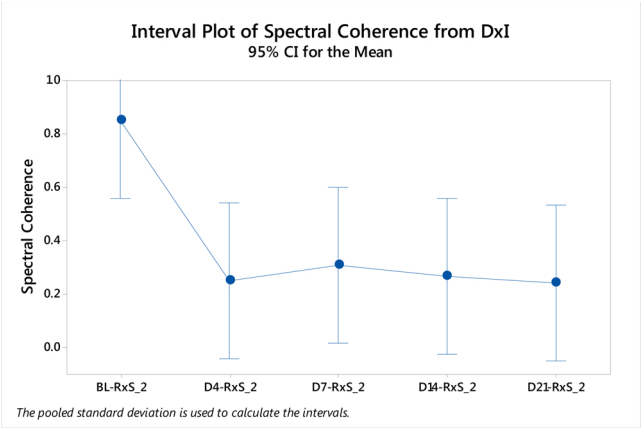

Fig. 6. Interval plot of the Spectral Coherence from the left hemisphere recording with right forelimb and hindlimb simulation of DxI vs days before and after injury with a 95 % confidence interval.

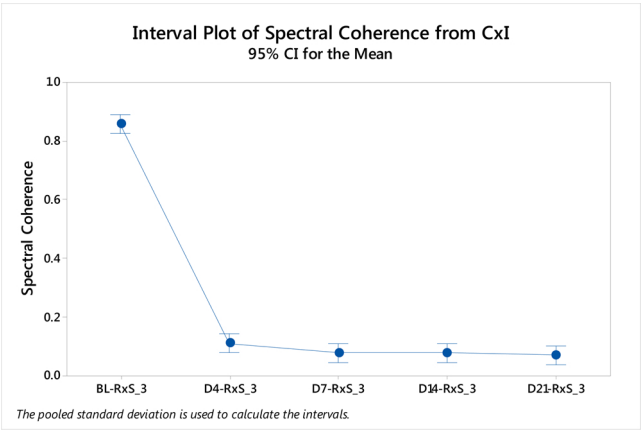

Fig. 7. Interval plot of the Spectral Coherence from the left hemisphere recording with right forelimb and hindlimb simulation of CxI vs days before and after injury with 95 % confidence interval.

statistical significant difference between the means before or after injury as shown in Table 5.

We then repeated the same analysis on spectral coherence data obtained from all animals with DxI and CxI. Figs. 6 and 7 show the interval plot of the spectral coherence from the left hemisphere recording with right forelimb and right hindlimb simulation of RxI vs days before and after injury with a 95 % confidence interval. Results demonstrated that there is a significant difference between these means ($p = 0.02$) for DxI and ($p = 0.00$) for CxI and hence reject the hypothesis of equal means.

We have also created grand average for each animal for the forelimb and hindlimb SSEPs. Fig. 8 shows examples of the grand average from individual animals of each group at baseline and D21.

4. Discussion

The prime objective of this investigation was to study the feasibility of using forelimb SSEP signals as a practical alternative to baseline data for the assessment of thoracic spinal cord injury. In real life, for patients with SCI, baseline SSEPs are obviously unavailable and thus rendering useless any diagnosis or treatment assessment methods that rely on baseline signals. Although forelimb and hindlimb SSEP signals do not have an identical shape, there is always a high degree of correlation between them when the applied stimulations are identical and have the same electrical parameters and source.

Our second objective was to investigate the possibility of using the spectral coherence as a quantitative measure to reflect the severity of SCI. The advantages of using this technique include; (i) practicality to obtain a normalized, objective, and quantitative measure with values ranging between 0 and 1, (ii) not requiring trained examiners, and (iii) feasibility of using the forelimb SSEP signals of any day following the injury and hence, overcoming the need for baseline hindlimb SSEP.

Results obtained from all animals, regardless of the modality (location and severity) of their injury in the thoracic area, show that spectral coherence before the injury is constantly above 0.8, but it always drops below 0.7 (in a scale between 0 and 1) following the injury. This can be reliably considered as an indicator of both onset of injury and the severity of the injury. Based on the results reported above, we conclud that Rxl is the least severe and Cxl is the most severe transection injury. It is noteworthy that we also obtained similar results with the contusion model of thoracic SCI as well (Al-Nashash et al., 2009).

In addition, we performed a simple main-effect analysis of variance test before and after the injury. The null hypothesis of equal spectral coherence means on different days demonstrated that there is a significant difference between these means ranging between “mild” right transection injury with $p = 0.05$ and “moderate to severe” double hemi transection with $p = 0.02$ and “very severe” complete transection with $p = 0.00$ respectively.

The above results demonstrate that global spectral coherence between forelimb and hindlimb signals can be used as a quantitative measure to detect the onset and assess the degree of severity of spinal cord injury. In addition, we determined that the spectral coherence values below 0.3 indicate severe thoracic spinal cord injury.

In conclusion, this study validates the potential of SSEP usage for SCI monitoring in transection SCI. As we previously reported (All et al., 2019), the histological results and the outcome from motor behavioral scoring analysis (data not reported here to avoid repetition) quantifying the injury severity of each animal and allow us to conclude that the global spectral coherence between forelimb and hindlimb signals can be used as a quantitative measure to detect the onset and assess the degree of severity of spinal cord injury. Ours, as well as others’ previous studies, have shown that in rodent models of both transection and contusion SCI, spectral coherence analysis of SSEP can provide an adequate assessment of SCI progression and rehabilitation, especially for hindlimb (Fatoo et al., 2007). Since the transection and contusion models combined accounts for the majority of human SCI cases (Cheriyan et al., 2014; Young, 2002), the adoption of the proposed analysis of SSEP in the detection and monitoring of SCI would empower healthcare providers and offer objectivity assessments and standardization. By extending the usage of spectral coherence method to transection model of SCI, this investigation provides researchers more options in their studies of SCI, especially in evaluating potential neuroprotective measures (Teh et al., 2018). As a continuous and sensitive monitoring modality, SSEP would also enable us to investigate neuroplasticity and neural reorganization (All et al., 2012).

Author contribution

Angelo All (A.A.) and Hasan Al Nashash (H.A.) contributed to the conception and experimental design. H.A. completed data analysis. A.A., H.A. and Shiyu Luo (S.L.) drafted the paper. A.A. and S.L. performed literature search. A.A., H.A. and Xiaogang Liu (X.L.) supervised and provided critical revision.

Funding

This research project was partially supported by the Hong Kong Baptist University (HKBU) grant: 31.4531.179234 (Faculty Seed Fund, PI: A. H. All) and grant: 21.4531.162640 (Start-Up Tier 1 Fund, PI: A. H. All).

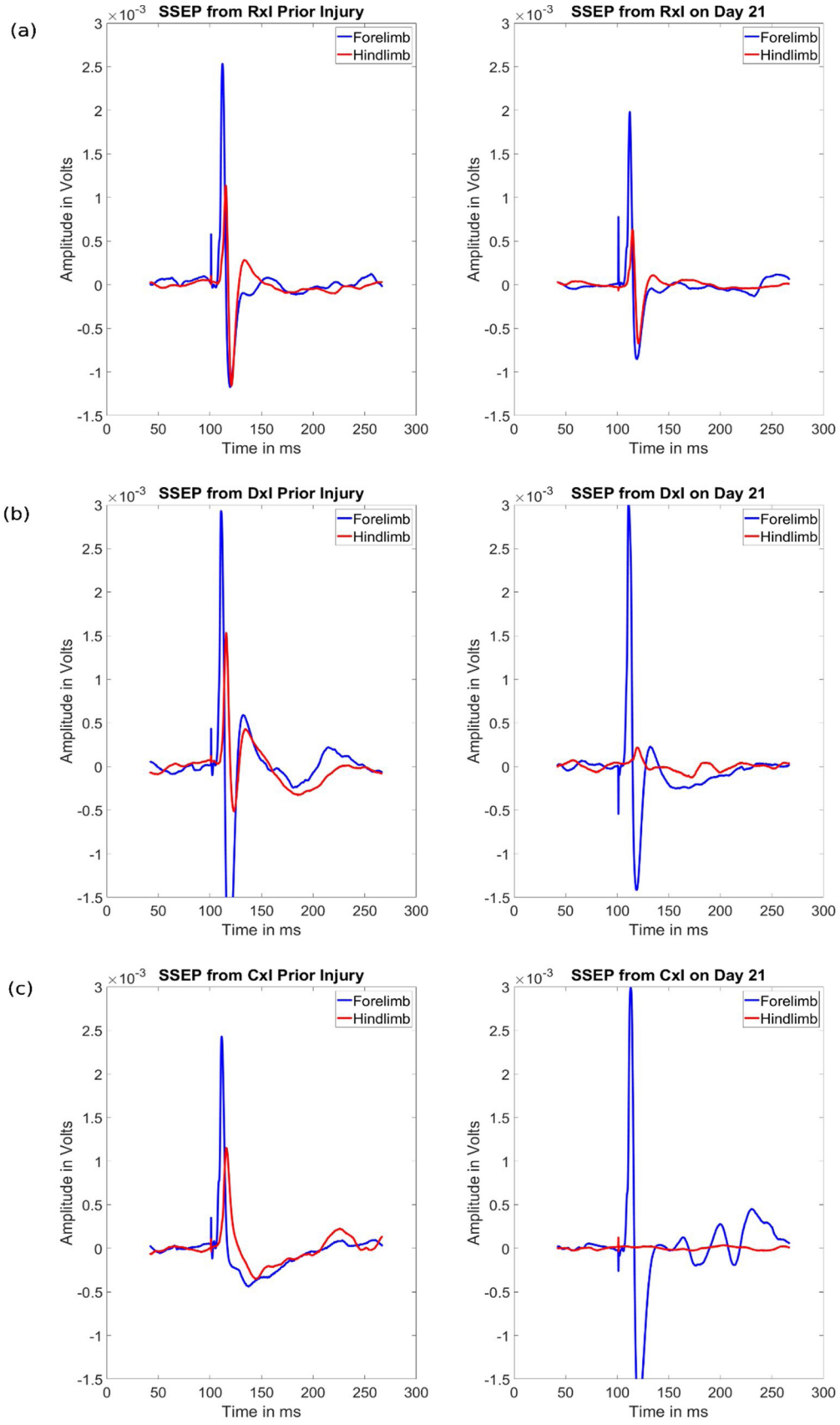

Fig. 8. The grand average from individual animals from each group at baseline and D21 – (a) RxI: BL and D21; (b) DxI: BL and D21 (c) CxI: BL and D21.

Declaration of Competing Interest

The authors declare that they have no conflict of interest.

Acknowledgment

We would like to thank Dr. Jukka Kortelainen, Dr. Janani Manivannan, Mr. Thow Xin Yuan, Ms. Astrid, Ms. Ashwati Vipin, and Ms. Chua Soo Min for their contribution in the experimental procedures, electrophysiology monitoring, animal care and administrative role in this project.

References

Agrawal, G., Sherman, D., Thakor, N., All, A., 2008. A novel shape analysis technique for somatosensory evoked potentials. Conference ProcEedings : Annual International Conference of the IEEE Engineering in Medicine and Biology SocietyIEEE Engineering in Medicine and Biology SocietyAnnual Conference. 2008 4688–4691.

Agrawal, G., Iyer, S., All, A.H., 2009. A comparative study of recording procedures for motor evoked potential signals. Conference Proceedings : Annual International Conference of the IEEE Engineering in Medicine and Biology SocietyIEEE Engineering in Medicine and Biology SocietyAnnual Conference. 2009 2086–2089.

Agrawal, G., Kerr, C., Thakor, N.V., All, A.H., 2010. Characterization of graded multicenter animal spinal cord injury study contusion spinal cord injury using somatosensory-evoked potentials. Spine 35 (11), 1122–1127.

Ahuja, C.S., Wilson, J.R., Nori, S., Kotter, M.R.N., Druschel, C., Curt, A., et al., 2017. Traumatic spinal cord injury. Nat. Rev. Dis. Primers 3, 17018.

Using spectral coherence for the detection and monitoring of spinal cord injury. In: All, A., Fatoo, N., Mirza, N., Ahmed, R., Al-Nashash, H., Thakor, N. (Eds.), GCC Ind Electr Electron Conf, Manama, Bahrain; 2007.

All, A.H., Agrawal, G., Walczak, P., Maybhate, A., Bulte, J.W., Kerr, D.A., 2010. Evoked potential and behavioral outcomes for experimental autoimmune encephalomyelitis in Lewis rats. Neurol. Sci. 31 (5), 595–601.

All, A.H., Bazley, F.A., Gupta, S., Pashai, N., Hu, C., Pourmorteza, A., et al., 2012. Human embryonic stem cell-derived oligodendrocyte progenitors aid in functional recovery of sensory pathways following contusive spinal cord injury. PLoS One 7 (10), e47645.

All, A.H., Al Nashash, H., Mir, H., Luo, S., Liu, X., 2019. Characterization of transection spinal cord injuries by monitoring somatosensory evoked potentials and motor behavior. Brain Res. Bull.

Al-Nashash, H., Fatoo, N.A., Mirza, N.N., Ahmed, R.I., Agrawal, G., Thakor, N.V., et al., 2009. Spinal cord injury detection and monitoring using spectral coherence. IEEE Trans. Biomed. Eng. 56 (8), 1971–1979.

Bazley, F.A., All, A.H., Thakor, N.V., Maybhate, A., 2011. Plasticity associated changes in cortical somatosensory evoked potentials following spinal cord injury in rats. Conference Proceedings : Annual International Conference of the IEEE Engineering in Medicine and Biology SocietyAnnual Conference. 2011 2005–2008.

Bazley, F.A., Pourmorteza, A., Gupta, S., Pashai, N., Kerr, C., All, A.H., 2012. DTI for assessing axonal integrity after contusive spinal cord injury and transplantation of oligodendrocyte progenitor cells. Conference Proceedings : Annual International Conference of the IEEE Engineering in Medicine and Biology Society Annual Conference. 2012 82–85.

Bazley, F.A., Maybhate, A., Tan, C.S., Thakor, N.V., Kerr, C., All, A.H., 2014. Enhancement of bilateral cortical somatosensory evoked potentials to intact forelimb stimulation following thoracic contusion spinal cord injury in rats. Ieee Trans. Neural Syst. Rehabil. Eng. 22 (5), 953–964.

Bernal, J., Baldwin, M., Gleason, T., Kuhlman, S., Moore, G., Talcott, M., 2009. Guidelines for rodent survival surgery. J. Investig. Surg. 22 (6), 445–451.

Cerutti, S., Chiarenza, S., Liberati, D., Mascellani, P., Pavesi, G.A., 1988. Parametric Method Of Identification Of Single-trial Event-related Potentials In The Brain. IEEE Trans. Biomed. Eng. 35 (9), 701–711.

Cheriyan, T., Ryan, D.J., Weinreb, J.H., Cheriyan, J., Paul, J.C., Lafage, V., et al., 2014. Spinal cord injury models: a review. Spinal Cord 52 (8), 588.

Detection and assessment of spinal cord injury using spectral coherence. In: Fatoo, N., Mirza, N., Ahmad, R., Al-Nashash, H., Naeini, H., Thakor, N. (Eds.), 2007 29th Annual International Conference of the IEEE Engineering in Medicine and Biology Society; 2007 IEEE.

Flecknell, P.A., 2016. Laboratory Animal Anaesthesia, 4th ed. Amsterdam; Boston: Elsevier/AP, Academic Press is an imprint of Elsevier xxvii, 321 pages p.

Grimm, K.A., Lamont, L.A., Tranquilli, W.J., Greene, S.A., Robertson, S.A., 2015. Veterinary Anesthesia and Analgesia, 5th ed. Wiley Blackwell, Ames, Iowa x, 1061 pages p.

Iyer, S., Maybhate, A., Presacco, A., All, A.H., 2010. Multi-limb acquisition of motor evoked potentials and its application in spinal cord injury. J. Neurosci. Methods 193 (2), 210–216.

Quantitative outcome measures for assessing motor control in a rodent model of spinal contusion injury. In: Jung, R., Knapp, E.A., Thota, A.K., Thompson, B.T., Mulligan, S., Ravi, N. (Eds.), Proceedings of the Second Joint 24th Annual Conference and the Annual Fall Meeting of the Biomedical Engineering Society][Engineering in Medicine and Biology; 2002 IEEE.

Kong, X., Thakor, N.V., 1996. Adaptive estimation of latency changes in evoked potentials. IEEE Trans. Biomed. Eng. 43 (2), 189–197.

Krause, J.S., Saunders, L.L., 2011. Health, secondary conditions, and life expectancy after spinal cord injury. Arch. Phys. Med. Rehabil. 92 (11), 1770–1775.

Lee, B.B., Cripps, R.A., Fitzharris, M., Wing, P.C., 2014. The global map for traumatic spinal cord injury epidemiology: update 2011. global incidence rate. Spinal cord. 52 (2), 110.

Maybhate, A., Hu, C., Bazley, F.A., Yu, Q., Thakor, N.V., Kerr, C.L., et al., 2012. Potential long term benefits of acute hypothermia after spinal cord injury: assessments with somatosensory evoked potentials. Crit. Care Med. 40 (2), 573.

Maynard, F.M., Bracken, M.B., Creasey, G., Ditunno, J.F., Donovan, W.H., Ducker, T.B., et al., 1997. International standards for neurological and functional classification of spinal cord injury. American spinal injury association. Spinal Cord 35 (5), 266–274.

Mir, H., Al-Nashash, H., Kerr, D., Thakor, N., All, A., 2010. Histogram based quantification of spinal cord injury level using somatosensory evoked potentials. Conference Proceedings : Annual International Conference of the IEEE Engineering in Medicine and Biology SocietyIEEE Engineering in Medicine and Biology SocietyAnnual Conference. 2010 4942–4945.

Spinal cord injury evaluation using morphological difference of somatosensory evoked potentials. In: Mir, H., Al-Nashash, H., Kerr, D., All, A., Thakor, N. (Eds.), 2011 5th International Conference on Bioinformatics and Biomedical Engineering; 2011 10-12 May.

Mir, H., Al-Nashash, H., Kortelainen, J., All, A., 2018. Novel modeling of somatosensory evoked potentials for the assessment of spinal cord injury. IEEE Trans. Biomed. Eng. 65 (3), 511–520.

New, P.W., Cripps, R.A., Lee, B.B., 2014. Global maps of non-traumatic spinal cord injury epidemiology: towards a living data repository. Spinal Cord 52 (2), 97.

Nuwer, M.R., 1998. Fundamentals of evoked potentials and common clinical applications today. Electroencephalogr. Clin. Neurophysiol. 106 (2), 142–148.

Sherman, D.L., Wuyyuru, V., Brooke, M.J., Zhang, H.X., Sepkuty, J.P., Thakor, N.V., et al., 2010. Spinal cord integrity monitoring by adaptive coherence measurement. J. Neurosci. Methods 193 (1), 90–99.

Teh, D.B.L., Chua, S.M., Prasad, A., Kakkos, I., Jiang, W., Yue, M., et al., 2018. Neuroprotective assessment of prolonged local hypothermia post contusive spinal cord injury in rodent model. Spine J. 18 (3), 507–514.

Vayrynen, E., Noponen, K., Vipin, A., Thow, X.Y., Al-Nashash, H., Kortelainen, J., et al., 2016. Automatic parametrization of somatosensory evoked potentials with chirp modeling. IEEE Trans. Neural Syst. Rehabil. Eng. 24 (9), 981–992.

Vipin, A., Thow, X.Y., Mir, H., Kortelainen, J., Manivannan, J., Al-Nashash, H., et al., 2016. Natural progression of spinal cord transection injury and reorganization of neural pathways. J. Neurotrauma 33 (24), 2191–2201.

Waynforth, H.B., 1980. Experimental and Surgical Technique in the Rat. Academic Press, London ; New York xv, 269 p. p.

Young, W., 2002. Spinal Cord Contusion Models. Progress in Brain Research. 137. Elsevier, pp. 231–255.